



# RESEARCH MEMORANDUM

EFFECTIVE MODULUS IN PLASTIC BUCKLING OF  
HIGH-STRENGTH ALUMINUM-ALLOY SHEET

By James A. Miller and Pearl V. Jacobs

National Bureau of Standards

NATIONAL ADVISORY COMMITTEE  
FOR AERONAUTICS

WASHINGTON  
September 20, 1951

NACA LIBRARY  
LAWRENCEVILLE, GEORGIA

NACA RM 51G11

## NATIONAL ADVISORY COMMITTEE FOR AERONAUTICS

## RESEARCH MEMORANDUM

EFFECTIVE MODULUS IN PLASTIC BUCKLING OF  
HIGH-STRENGTH ALUMINUM-ALLOY SHEET

By James A. Miller and Pearl V. Jacobs

## SUMMARY

Results of compressive tests on duplicate longitudinal specimens from sheets of 75S-T6 and R301-T aluminum alloys in three thicknesses are presented as graphs of tangent modulus  $E_t$ , secant modulus  $E_s$ , and  $\sqrt{\frac{1}{4} + \frac{3}{4} \frac{E_t}{E_s}}$  plotted against stress on a dimensionless basis.

These functions may be used to obtain values of the plasticity coefficients referred to in "A Unified Theory of Plastic Buckling of Columns and Plates" by Elbridge Z. Stowell (NACA Rep. 898). In Stowell's theory the critical stress computed for the elastic case is multiplied by the appropriate plasticity coefficient to give the critical stress for the plastic case.

## INTRODUCTION

It is customary, in computing critical stresses for columns stressed in the plastic range, to replace, in the Euler formula, Young's modulus  $E$  by an effective modulus  $E_0$ . Sometimes the tangent modulus  $E_t$  or the secant modulus  $E_s$  is used. From theoretical considerations, Stowell has proposed in reference 1 various effective moduli depending on the conditions of loading. These are given in dimensionless form in table 1 as  $\eta$ , the ratio by which the critical stress for the plastic case is to be multiplied to obtain the critical stress for the elastic case. (Also,  $\eta$  may be defined as the ratio of effective modulus to Young's modulus.) Values of  $\eta$  range from  $E_t/E$  to  $E_s/E$  with intermediate values determined from various combinations of the two and  $\sqrt{\frac{1}{4} + \frac{3}{4} \frac{E_t}{E_s}}$ .

The latter can also be used to find general expressions for the plasticity reduction factor  $\eta$  which apply to H-sections with certain dimensional ratios (reference 2).

This report shows graphs of  $E_t/E$ ,  $E_s/E$ , and  $\sqrt{\frac{1}{4} + \frac{3}{4} \frac{E_t}{E_s}}$  plotted against  $\sigma$ , the ratio of stress  $s$  to secant yield strength (0.7E)  $s_1$ , for compressive specimens loaded in the direction of rolling (longitudinal) from sheets of aluminum alloys 75S-T6 and R301-T in three thicknesses. The data from which these graphs were derived were reported in references 3 and 4.

Graphs for alclad sheet (references 5 to 8) are not included since the methods proposed by Stowell in reference 1 are not applicable when the clad coating is soft (see reference 9). Although aluminum-alloy R301-T sheet is clad, the cladding is a strong alloy of aluminum. It was assumed that for this material the cladding would be strong enough to make the methods of reference 1 approximately correct. However, the curves for the R301-T sheet can be expected to give values of critical buckling stress a little too high in the region from about  $\sigma = 0.4$  to 0.9, particularly for the thinner gages.

This project, conducted at the National Bureau of Standards, was sponsored by and conducted with the financial assistance of the National Advisory Committee for Aeronautics.

#### MATERIAL

The aluminum-alloy 75S-T6 sheet was obtained from the Aluminum Company of America. It was received in the heat-treated and artificially aged condition designated T (now T6). The sheet thicknesses were 0.032, 0.064, and 0.125 inch.

The aluminum-alloy R301-T sheet was obtained from the Reynolds Metals Company. It was received in the heat-treated and artificially aged condition designated by T. The sheet thicknesses were 0.020, 0.032, and 0.064 inch. The nominal thickness of cladding on each side amounted to 10, 7.5, and 5 percent, respectively, of the sheet thickness.

#### DATA

The data are shown in dimensionless stress-strain graphs in references 3 and 4. The data were obtained from tests made on two longitudinal (in direction of rolling) specimens from a sheet of each thickness. The specimens were rectangular strips 0.50 inch wide by 2.25 inches long.

The tests were made in a 50-kip capacity beam-and-poise screw-type testing machine using the 0 to 5 kip scale range. The specimens were tested between hardened-steel bearing blocks in the subpress described in reference 10. Lateral support against premature buckling was furnished by lubricated solid guides as described in reference 11. The strain was measured with a pair of 1-inch Tuckerman optical strain gages attached to opposite edge faces of the specimen. The rate of loading was about 2 ksi per minute.

#### GRAPHS

The graphs are shown in figures 1 to 6. They give curves of  $E_t/E$ ,  $E_s/E$ , and  $\sqrt{\frac{1}{4} + \frac{3}{4} \frac{E_t}{E_s}}$  plotted against  $\sigma$  where  $\sigma = s/s_1$ ,  $s$  is stress, and  $s_1$  is secant yield strength (0.7E). Values of  $s_1$  and  $E$  are given in the graphs. They are the averages of the experimental values for pairs of specimens as given in table 2. Each individual value of Young's modulus was taken as the slope of a least-squares straight line fitted to the stress-strain curve below the beginning of the knee.

The tangent-modulus curves were each fitted to a plot of ratios of increment in  $\sigma$  to increment in  $\epsilon$  ( $\epsilon = \text{Strain} \times E/s_1$ ) for successive points, each plotted against the average value of  $\sigma$ . The tangent-modulus curves in figures 1, 2, and 3 are those shown in figures 15, 17, and 19, respectively, of reference 3. The tangent-modulus curves in figures 4, 5, and 6 are faired through values plotted from the data used in preparing the compressive stress-strain curves shown in figures 1, 8, and 15, respectively, of reference 4. Individual measured values are not shown in figures 1 to 6; however, they differed from the faired curves by less than 0.03 in  $E_t/E$  except for a few points on each curve where the measured values differed from the faired curves shown by as much as 0.1. An indication of the fit of the curves to the points can be obtained from the graphs of tangent modulus in references 3 and 4. The values of tangent modulus increased with  $\sigma$  in the elastic range, the initial value being a little below the average determined by least squares.

The secant-modulus curves were each fitted to a plot of ratios of  $\sigma$  to  $\epsilon$  plotted against  $\sigma$ . Secant- and tangent-modulus curves were drawn through a common origin. The secant-modulus graph has less slope than the tangent-modulus graph at low values of  $\sigma$ .

The  $\sqrt{\frac{1}{4} + \frac{3}{4} \frac{E_t}{E_s}}$  curves were plotted from values calculated from corresponding values of  $E_t/E$  and  $E_s/E$  obtained from the curves.

These curves started at 1 for  $\sigma = 0$  and rose slightly at low values of  $\sigma$ .

#### EXAMPLE

A long plate of aluminum-alloy 75S-T6 sheet, having a thickness  $h$  of 0.1875 inch, a width  $b$  of 4 inches, a modulus of elasticity in compression  $E$  of 10,500 ksi, and a secant yield strength  $(0.7E)$   $s_1$  of 72 ksi, is loaded in compression at the ends with the unloaded edges simply supported. It is desired to estimate the critical buckling stress  $s_{cr}$  of the plate.

For the elastic case, Timoshenko (reference 12, p. 331) gives

$$s_{cr} = \frac{k\pi^2 E h^2}{12(1 - \nu^2)b^2} \quad (1)$$

where  $k$  is a constant depending on the plate dimensions and  $\nu$  is Poisson's ratio. In the plastic range,  $E$  is replaced by the effective modulus  $E_e$  giving

$$s_{cr} = \frac{k\pi^2 E_e h^2}{12(1 - \nu^2)b^2} \quad (1a)$$

Setting  $\sigma_{cr} = s_{cr}/s_1$  and taking  $k = 4$  for a long simply supported plate,  $\nu = 1/3$ , and the other numerical constants as previously given, equation (1a) can be written as

$$\sigma_{cr} = 3.70 \frac{E_e}{s_1} \frac{h^2}{b^2} \frac{E_e}{E} = 1.186 E_e/E \quad (2)$$

This line is plotted as the dashed line in figure 7. The value of  $\sigma$  for which  $\sigma = 1.186 E_e/E$  is the buckling value  $\sigma_{cr}$ . To determine this value a curve of  $E_e/E$  against  $\sigma$  must be plotted. For the condition of loading in this example, table 1 gives the following relation for computing  $E_e/E$  from  $E$ ,  $E_s$ , and  $E_t$ :

$$\frac{E_e}{E} = \frac{E_s}{E} \left( \frac{1}{2} + \frac{1}{2} \sqrt{\frac{1}{4} + \frac{3}{4} \frac{E_t}{E_s}} \right) \quad (3)$$

Taking the values of  $E_s/E$  and  $E_t/E_s = (E_t/E)/(E_s/E)$  from figure 3, for the best approximation to the material used in this example, the value of  $E_e/E$  was computed for two values of  $\sigma$ . These values are

shown as points in figure 7. The curve joining these points intersects the dashed line representing equation (2) at the value  $\sigma$  equal to  $\sigma_{cr} = 0.91$ . Portions of the curves of  $E_s/E$  and  $\sqrt{\frac{1}{4} + \frac{3}{4} \frac{E_t}{E_s}}$  from figure 3 were plotted to assist in choosing values of  $\sigma$  in the neighborhood of  $\sigma_{cr}$  for the detailed computations. Since  $\sigma_{cr} = s_{cr}/s_1$

$$s_{cr} = s_1 \sigma_{cr} = 72 \text{ ksi} \times 0.91 = 65.5 \text{ ksi}$$

which is the critical buckling stress that was to be estimated.

National Bureau of Standards  
Washington, D. C., February 12, 1951

## REFERENCES

1. Stowell, Elbridge Z.: A Unified Theory of Plastic Buckling of Columns and Plates. NACA Rep. 898, 1948. (Formerly NACA TN 1556.)
2. Stowell, Elbridge Z., and Pride, Richard A.: Plastic Buckling of Extruded Composite Sections in Compression. NACA TN 1971, 1949.
3. Miller, James A.: Stress-Strain and Elongation Graphs for Aluminum-Alloy 75S-T6 Sheet. NACA TN 2085, 1950.
4. Miller, James A.: Stress-Strain and Elongation Graphs for Aluminum Alloy R301 Sheet. NACA TN 1010, 1946.
5. Miller, James A.: Stress-Strain and Elongation Graphs for Alclad Aluminum-Alloy 75S-T Sheet. NACA TN 1385, 1947.
6. Miller, James A.: Stress-Strain and Elongation Graphs for Alclad Aluminum-Alloy 24S-T Sheet. NACA TN 1512, 1948.
7. Miller, James A.: Stress-Strain and Elongation Graphs for Alclad Aluminum-Alloy 24S-T81 Sheet. NACA TN 1513, 1948.
8. Miller, James A.: Stress-Strain and Elongation Graphs for Alclad Aluminum-Alloy 24S-T86 Sheet. NACA TN 2094, 1950.
9. Buchert, Kenneth P.: Stability of Alclad Plates. NACA TN 1986, 1949.
10. Aitchison, C. S., and Miller, James A.: A Subpress for Compressive Tests. NACA TN 912, 1943.
11. Miller, James A.: A Fixture for Compressive Tests of Thin Sheet Metal between Lubricated Steel Guides. NACA TN 1022, 1946.
12. Timoshenko, S.: Theory of Elastic Stability. First ed., McGraw-Hill Book Co., Inc., 1936.

TABLE 1.-RATIOS OF EFFECTIVE MODULUS TO YOUNG'S  
MODULUS FOR COLUMNS AND PLATES UNDER VARIOUS  
CONDITIONS OF LOADING (FROM REFERENCE 1)

[E, Young's modulus;  $E_t$ , tangent modulus;  $E_s$ , secant modulus;  
 $E_e$ , effective modulus;  $l$ , length;  $b$ , width]

Structure	$\eta = \frac{E_e}{E}$
Long flange, one unloaded edge simply supported	$\frac{E_s}{E}$
Long flange, one unloaded edge clamped	$\frac{E_s}{E} \left( 0.330 + 0.670 \sqrt{\frac{1}{4} + \frac{3}{4} \frac{E_t}{E_s}} \right)$
Long plates, both unloaded edges simply supported	$\frac{E_s}{E} \left( \frac{1}{2} + \frac{1}{2} \sqrt{\frac{1}{4} + \frac{3}{4} \frac{E_t}{E_s}} \right)$
Long plate, both unloaded edges clamped	$\frac{E_s}{E} \left( 0.352 + 0.648 \sqrt{\frac{1}{4} + \frac{3}{4} \frac{E_t}{E_s}} \right)$
Short plate loaded as a column, $\frac{l}{b} \ll 1$	$\frac{1}{4} \frac{E_s}{E} + \frac{3}{4} \frac{E_t}{E}$
Square plate loaded as a column, $\frac{l}{b} = 1$	$0.114 \frac{E_s}{E} + 0.886 \frac{E_t}{E}$
Long column, $\frac{l}{b} \gg 1$	$\frac{E_t}{E}$

TABLE 2.-EXPERIMENTAL VALUES OF YOUNG'S  
MODULUS AND SECANT YIELD STRENGTH

Specimen	Young's modulus, E (ksi)	Secant yield strength (0.7E), s <sub>1</sub> (ksi)
758-T6		
032-C1L	10,650	74.9
032-C2L	10,650	75.1
Average	10,650	75.0
064-C1L	10,630	71.9
064-C2L	10,640	72.8
Average	10,630	72.3
125-C1L	10,570	77.2
125-C2L	10,580	77.5
Average	10,570	77.3
R301-T		
020-C1L	10,780	61.4
020-C2L	10,770	61.2
Average	10,780	61.3
032-C1L	10,750	64.6
032-C2L	10,740	64.5
Average	10,750	64.6
064-C1L	10,790	62.1
064-C2L	10,800	62.2
Average	10,790	62.1



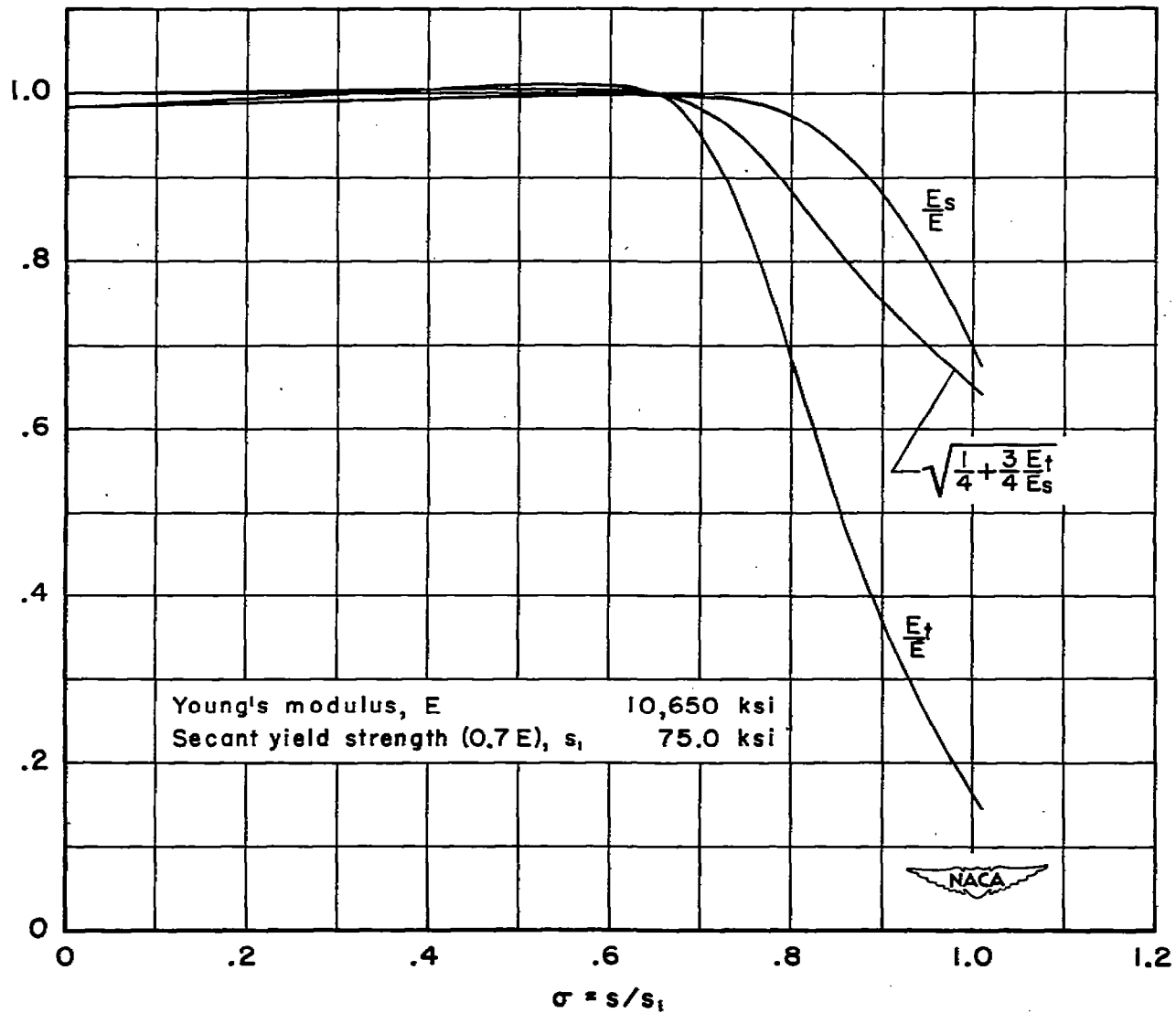


Figure 1.- Dimensionless graphs for estimating plastic buckling stress for aluminum-alloy 75S-T6 sheet 0.032 inch thick.

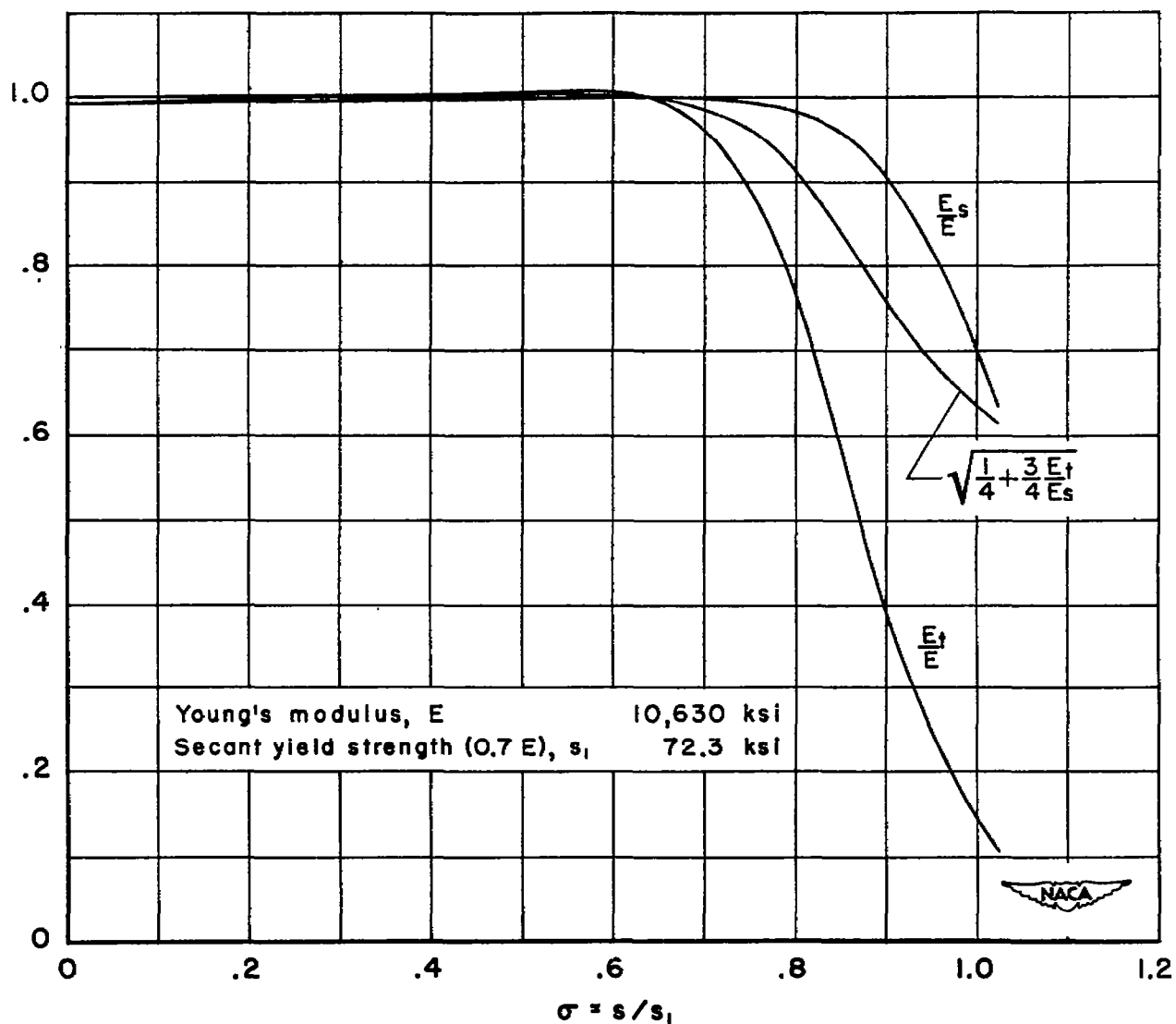


Figure 2.- Dimensionless graphs for estimating plastic buckling stress for aluminum-alloy 75S-T6 sheet 0.064 inch thick.

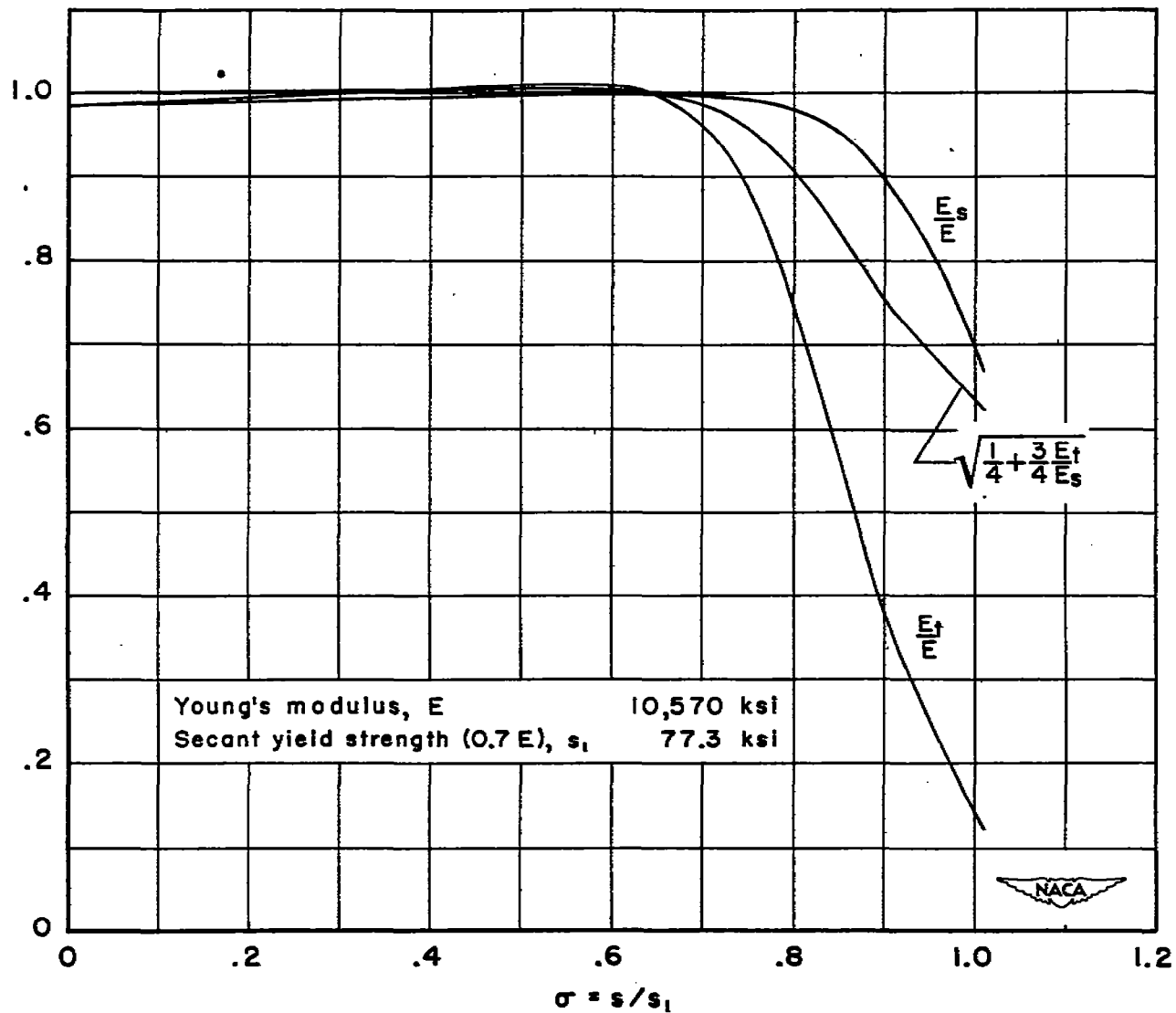


Figure 3.- Dimensionless graphs for estimating plastic buckling stress for aluminum-alloy 75S-T6 sheet 0.125 inch thick.

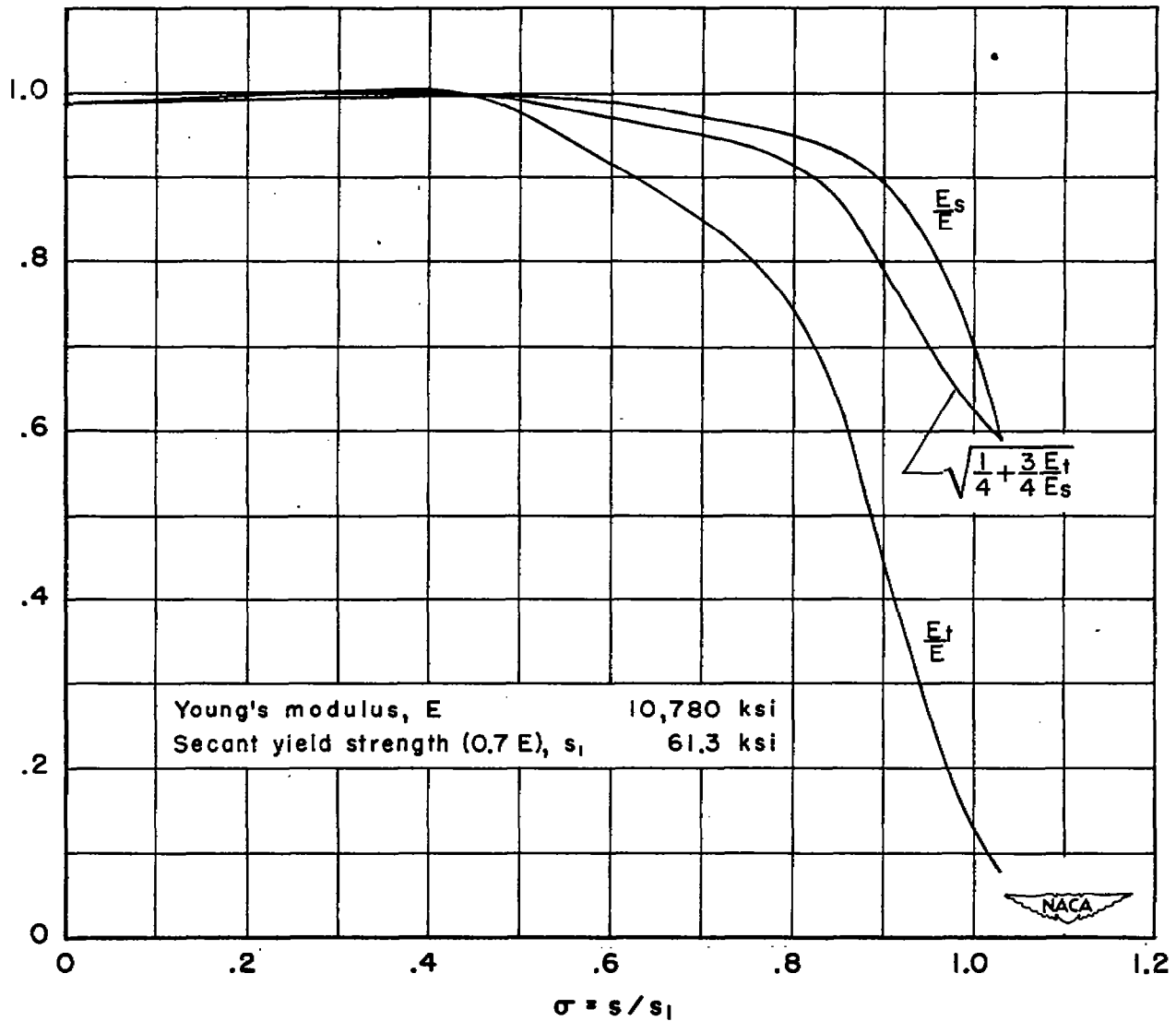


Figure 4.- Dimensionless graphs for estimating plastic buckling stress for aluminum-alloy R301-T sheet 0.020 inch thick.

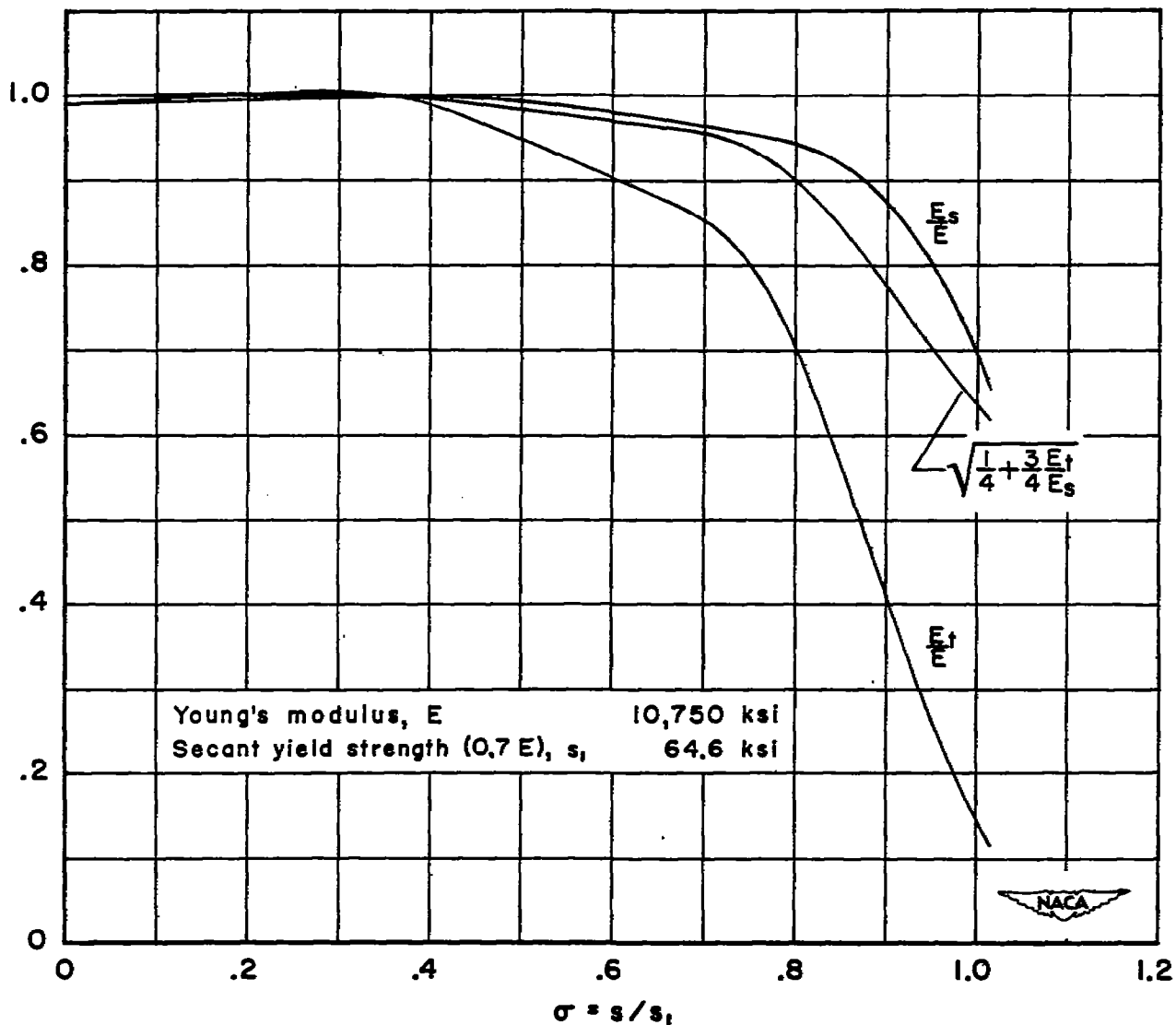


Figure 5.- Dimensionless graphs for estimating plastic buckling stress for aluminum-alloy R301-T sheet 0.032 inch thick.

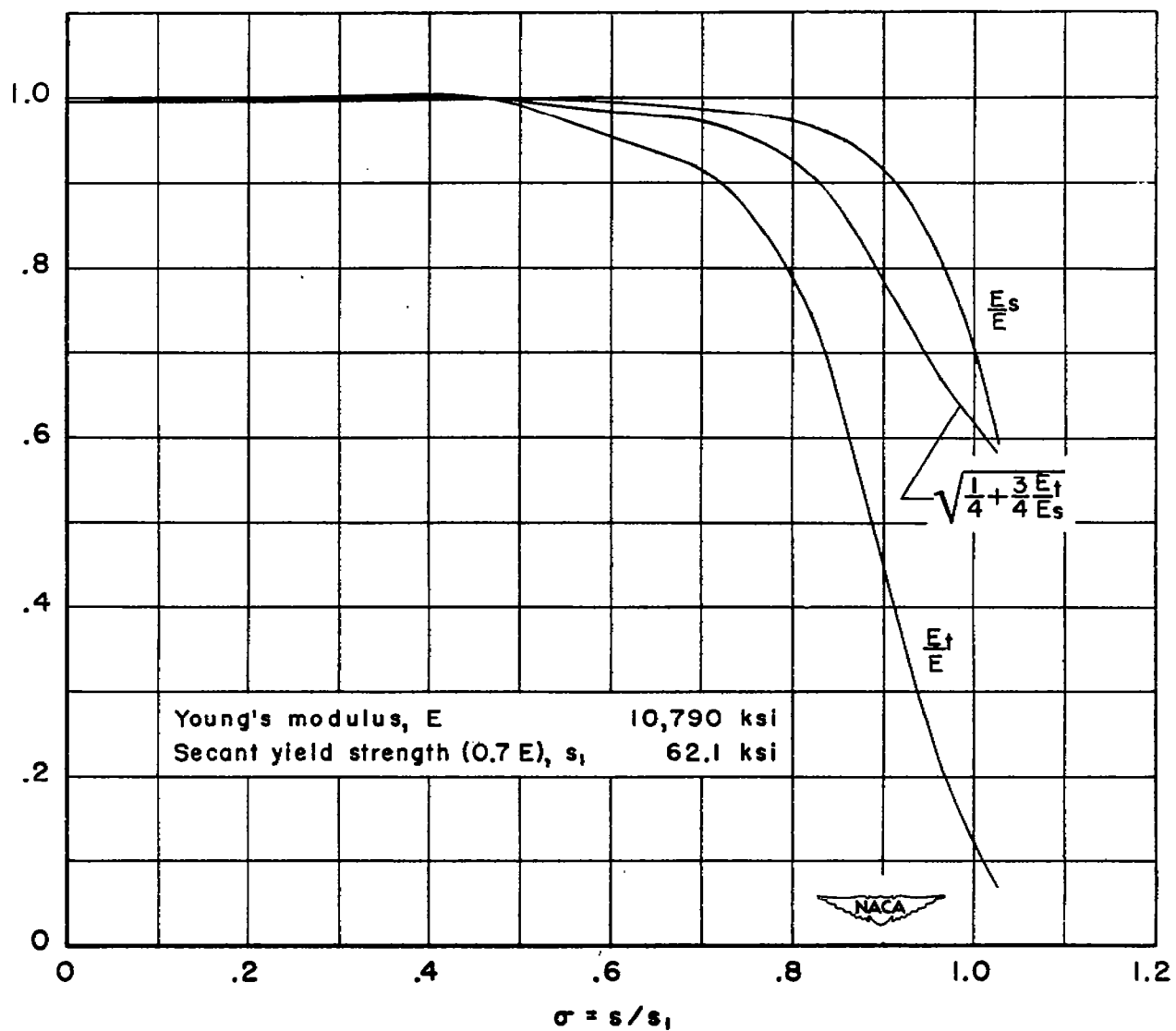


Figure 6.- Dimensionless graphs for estimating plastic buckling stress for aluminum-alloy R301-T sheet 0.064 inch thick.

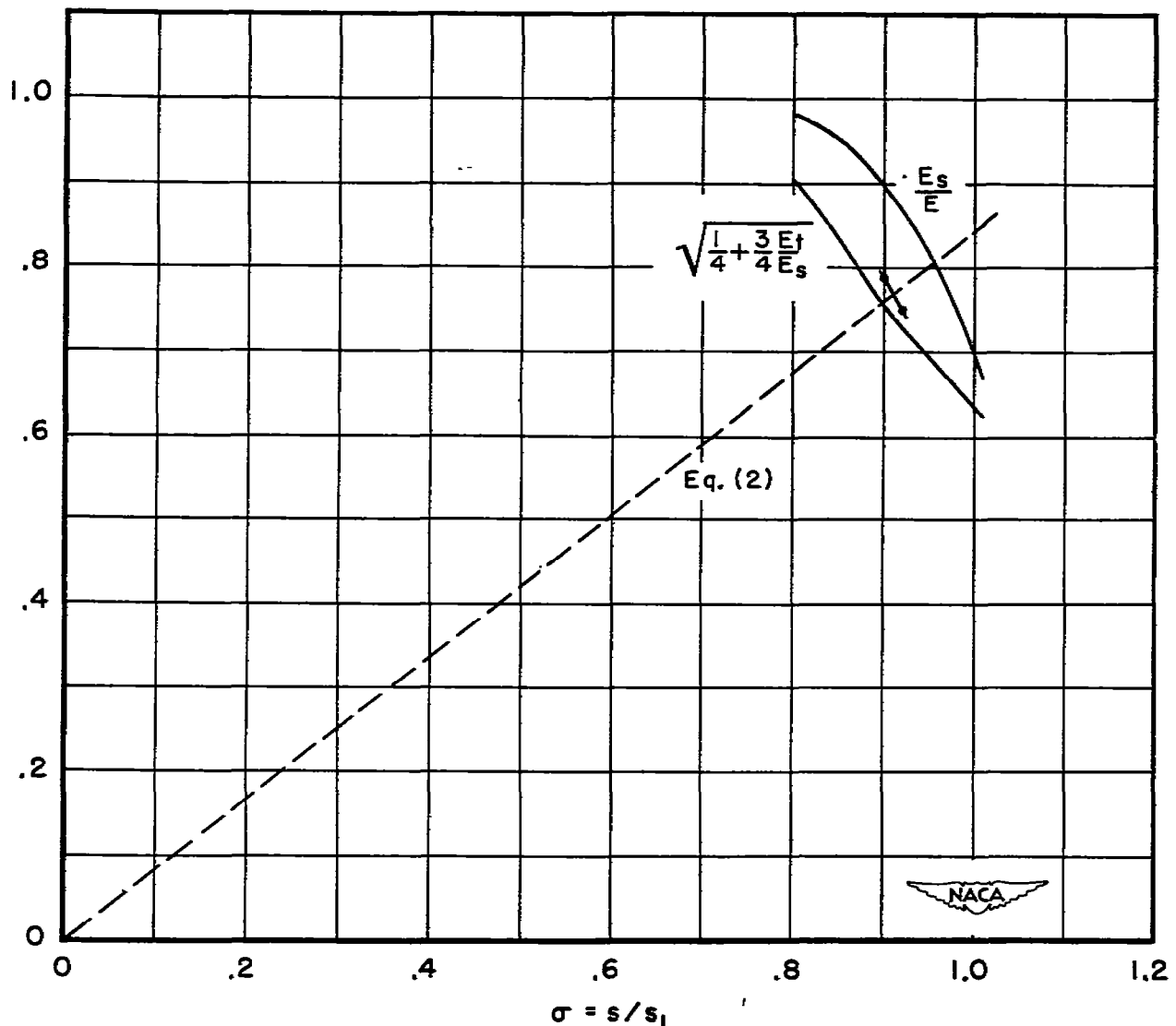


Figure 7.- Dimensionless graph illustrating use of Figure 3 in estimating buckling strength of a long plate with simply supported edges.

NASA Technical Library



3 1176 01434 3769